Improved Consequence Modelling for Hypothetical Accidents in Fusion Power Plants

W. E. Han

Euratom/UKAEA Fusion Association, Culham Science Centre, Abingdon, Oxfordshire, OX14 3DB, Tel.: +44 1235 528822
e-mail: winston.han@ukaea.org.uk

Abstract

Refinements to consequence modelling for hypothetical accidents in Fusion Power Plants have been explored. This leads to improved accuracy and a reduction in some of the conservatism inherent in previous calculations. Assumptions made in previous analyses for the Safety and Environmental Assessment of Fusion Power (SEAFP) are examined, with particular emphasis given to aerosol modelling within the containment and dispersion and dose calculations. By employing a more realistic treatment of the time dependence in the aerosol model and introducing a procedure for accounting for the effects of wind meander, it is shown how to obtain results which may be used to adjust previously derived dose estimates. Further analysis assesses the possibility of aerosol particle removal by filtering in cracks in the containment barriers, as material leaks into the environment. The potential for mitigation by this mechanism has been neglected in previous calculations.

1. INTRODUCTION

In this paper we examine consequence modelling for a hypothetical accident in a conceptual Fusion Power Plant (EU Power Plant Conceptual Study (PPCS)[1]). We consider a hypothetical worst case scenario in which an in-vessel loss of coolant accident (LOCA) could initiate a chain of events leading to release to the environment of some material containing radioactive components, and explore some refinements to the calculations designed to remove some conservatism.

The hypothetical containment system envisaged is that of an expansion volume surrounded by a containment building. Previous calculations[2,3] assumed that the whole source term for the mobilised material occupied the expansion volume at time zero but, in reality, it would take several hours or days to build up[4] via entry from the vacuum vessel. Also, dispersion calculations for the material reaching the external environment neglected wind meander. Taken together, these assumptions are conservative overall and, in section 2, we explore the consequence of relaxing them. The potential for removal of aerosol particles by filtering through cracks in containment barriers, also previously neglected, is addressed in section 3.

2. FINITE ENTRY TIME AND WIND MEANDER

2.1 Aerosol Modelling

In this section we account for the finite time taken for the aerosol to enter the expansion volume (entry time). Calculations have previously been presented using a model which, though monodisperse and with fixed size particles, was able to effectively describe the characteristics of the resulting polydisperse aerosol with good accuracy for the assumed conditions.[5,6] In order to describe the evolution of the aerosol with non-zero entry time, this model has been adapted so that the particle size can vary with time, although still monodisperse. This modelling will be described in more detail in reference 7.

The parameters used are chosen to reflect the conditions applicable to SEAFP analyses[2,3] ($V_1 = 6\text{x}10^4$ m^3, $V_2 = 1.4\text{x}10^5$ m^3, $l_1 = l_2 = 1/\tau_L$, $\tau_L = 100$ hours, $\rho = 3500$

kg m^{-3}, where ρ is the aerosol particle density and l_1 and V_1 are the leak-rate and volume of the expansion volume respectively, while l_2 and V_2 are those corresponding to the containment building). In figure 1 we present results for two values (100 and 1000 kg) of cumulative total injected aerosol mass. What these results show is that the total mass of aerosol released to the environment increases as the entry time is increased. This effect, which is strongest for the larger cumulative total injected aerosol mass, arises because the peak airborne mass diminishes with entry time, hence aerosol agglomeration rate and removal by gravitational settling also diminishes with entry time.

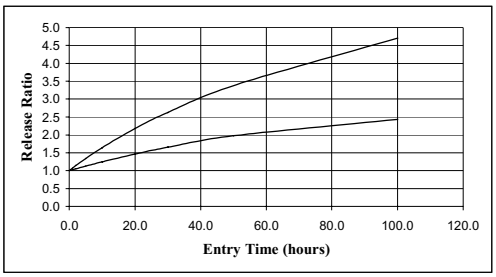

Figure 1. Curves of aerosol release ratio versus expansion volume entry time of aerosol vapour, for two values of cumulative total injected aerosol mass, 100kg (lower curve) and 1000kg (upper curve). Release ratio is defined as the ratio of aerosol mass released to that released for zero entry time.

2.2 Atmospheric Dispersion and Dose Calculations

We employ the widely used Gaussian Plume model to estimate the concentration of material in the plume of released aerosol carried by wind to the most exposed individual (MEI). This concentration, and therefore the dose to the MEI, is inversely proportional to both the vertical and horizontal spread of the plume, quantified by σ_z and σ_y, the standard deviations of the vertical and horizontal plume concentration profiles (assumed to be Gaussian). We now take account of wind meander by re-expressing the horizontal standard deviation[8] as:

$$\sigma_y^2 = \sigma_{yt}^2 + \sigma_{yw}^2$$

where σ_{yt} and σ_{yw} are the standard deviations due to turbulence and wind fluctuations respectively. The turbulent component is the basic short-duration dispersion parameter previously used, and the component due to fluctuations in wind direction may be approximated[8] by the following form:

$$\sigma_{yw} = 0.065\sqrt{\frac{7T}{u_{10}}}x$$

where T is the release duration in hours, u_{10} is the wind speed at height 10 m, and x is distance downwind from point of release in m. For a given total release, this formulation clearly leads to decreasing concentration and dose with increasing release duration.

2.3 Combined Results

Although not documented above, the finite entry time modelling leads to the result that release duration increases with entry time. Thus we can combine the release ratio results of the aerosol modelling with the wind meander analysis to obtain an overall correction factor which can be used to convert uncorrected results into values which take account of both finite entry time and wind meander.

We are interested in conditions relevant to previous SEAFP analyses, and assume there is a 0.5 km/hour wind blowing towards the MEI situated at the site boundary, 1 km from the containment building. The value of σ_{yt} employed corresponds to Pasquill weather category F, in order to produce a worst case estimate, and also takes into account building wake effects. Graphs of the correction factor versus aerosol entry time for two values of cumulative total injected aerosol mass are shown in figure 2.

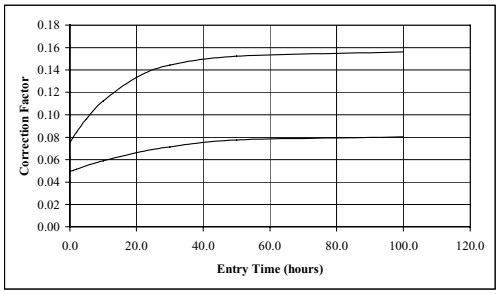

Figure 2. Curves of net correction factor versus expansion volume entry time of aerosol vapour, for two values of cumulative total injected aerosol mass, 100kg (lower curve) and 1000kg (upper curve).

The above analysis concerns the aerosol component of material mobilised during a hypothetical accident. The gaseous components of the mobilised material are not directly affected by the aerosol dynamics, but wind meander will have a considerable mitigative effect which undergoes no cancellation by finite entry time effects as in the case of the aerosol.

3. PARTICLE FILTERING BY CRACKS IN CONTAINMENT BARRIERS

The flow conditions modelled in the cracks correspond to the beginning of the leak calculations above. Time dependent aspects, such as deposition build-up and crack-plugging, will be dealt with in a subsequent analysis, and are not modelled here. The method is outlined below, and a more complete account will be found in reference 7. There are three main aspects to this problem: (i) estimating maximum separation of the crack walls, or centre crack opening displacement (COD), under accident conditions, (ii) defining the crack morphology and determining the gas flow as a function of COD, (iii) determining the rate of particle deposition in the cracks. These topics are dealt with in the following three sections, and specific cases are examined in the fourth.

3.1 Estimating the COD

In order to obtain estimates for upper and lower bounds of the COD, we have formulated the following approach. It is assumed that the barrier leak rate is known for the accident conditions, and that the actual gas flow and particle retention performance of the through cracks can be reasonably well characterised by a single typical crack size. A crack is opened up by stresses arising from the pressure difference across the barrier, and we can therefore estimate the COD for any crack width, given elasticity data for the barrier material and the simplifying assumption of spherical barrier geometry. Since we are also able to calculate flow rate for a given COD, we can estimate the number of cracks implied. In this way we have derived bounds assuming there will not be less than ten cracks (upper COD limit), and that the crack width will not be less than the barrier thickness (lower COD limit).

3.2 Crack Morphology and Gas Flow

The crack morphology model is based on that of Boussa et al[9] with parameters adjusted to suit the material. For the purpose of modelling the gas flow, the crack geometry is taken to be both uniform and infinite in the Z direction, parallel to the barrier surface. But, while predominantly following the X direction, which is normal to the barrier surface, the direction of the crack will tend to meander in the XY plane. The route taken by the gas flow through the crack can thus be represented by a series of linear segments whose lengths form a normal distribution. The angular orientations of the segments, with respect to some reference direction, are also normally distributed. The COD in the Y direction is assumed to be uniform throughout the crack. It is necessary to distinguish between the angular orientation of a line segment and the angular deviation of a bend. Given the angular distribution of all the line segments, which defines the crack morphology, we can obtain the distribution of the set of bends as a function of angular deviation if we take the segment orientations to be uncorrelated. It can be shown[7] that this assumption implies that $\sigma_\alpha = \sqrt{2}\ \sigma_\theta$ where σ_α and σ_θ are the standard deviations of the angular deviation and the segment orientation distributions, respectively.

For the scenarios examined in this paper (i.e., within the expected COD range), it turns out that, at the highest velocities, the dominant term balancing the pressure drive term in the energy equation for the flow is the energy loss due to the tortuosity of the path through the crack. Thus the limitation on flow velocity imposed by the crack morphology ensures that the flow remains laminar. In these circumstances, there is no turbulent particle deposition at the walls of the cracks, and the only significant deposition mechanism is that of inertial impaction arising at the points where the flow direction bends significantly. This arises when particles are too large to follow curved flow lines sufficiently closely to avoid hitting the wall.

3.3 Inertial Impaction

In order to determine the rate of particle impaction on the wall at a given bend, an expression for the impaction efficiency (the fraction of particles reaching the bend which hit the wall) as a function of the angular deviation (or change of flow direction) of a bend has been derived, and further details will be found in reference 7. Combining this information with an appropriate sticking probability for particles impacting the walls of the crack, enables calculation of the fraction of particles which are removed from the gas flow by inertial impaction. This can be quantified by a transmission factor representing the fraction of particles which pass right through the crack.

It is found that, for given crack parameters and flow conditions, there is a critical particle size below which there is no attenuation, and all particles get through. Above this critical value the transmission factor decreases sharply with size, rapidly approaching a constant pedestal value, T_p. For some scenarios considered, T_p can be extremely small (e.g., 10^{-5} – 10^{-40}) and this can be taken to indicate an effective particle size cutoff. However, in one scenario considered, T_p can approach 1. In the following section, a particle size cutoff curve actually represents the size for which the transmission factor is 0.1 (except when $1.05\ T_p > 0.1$, in which case it represents the size for which $T = 1.05\ T_p$).

3.4 Particle Filtering in Expansion Volume

The particle filtering effect has been examined for the case of leakage across the walls of an expansion volume. Conditions chosen are typical of those assumed for SEAFP analyses,[2,3] and the gas parameters assumed inside the expansion volume are appropriate for the helium-air mixture, at two atmospheres, resulting from blowdown following a LOCA in a helium cooled power plant design. Three alternative options for the wall material and thickness have been considered: (i) 6 mm steel, (ii) 6 cm steel, (iii) 0.5 m concrete.

3.4.1 Steel 6 mm

This case is relevant to a design of expansion volume in which the internal surfaces of the walls are covered with a steel liner. This analysis assumes a leak rate of 1% per day at 1 atmosphere overpressure and does not take into consideration any filtering which may arise in cracks in the supporting wall.

Figure 3 shows the particle size cutoff and transmission factor (the pedestal, or maximum attenuation, value) as a function of COD for such a barrier. Since transmission never falls much below 20% this is merely a partial cutoff. Furthermore, nearly all the cutoff curve falls between 2 and 3 micron, which is around the upper end of the range of the mass median diameter expected in scenarios explored. This would appear to suggest that, in many cases of interest, there is unlikely to be significant filtering. However, taking account of the reinforcing effect of the supporting walls of the expansion volume (assumed to be 0.5 m thick concrete) the procedure outlined above for estimating COD supplies a range of 1.9×10^{-6} – 5.8×10^{-5} m for the expected COD in the steel lining, giving rise to the possibility that the actual COD might be of the order of the particle size. If this is so, the validity of some assumptions break down, and the particles may be too large to pass through the crack. However, at present, there is no firm basis for claiming credit for particle filtering by a steel liner with the characteristics assumed.

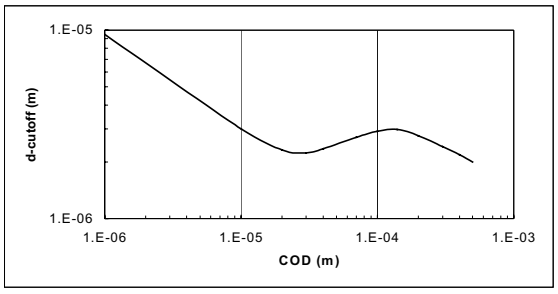

(a)

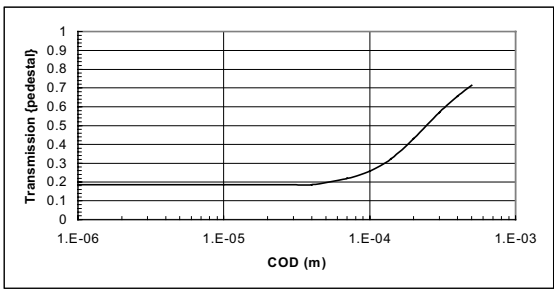

(b)

Figure 3. (a) Particle size cutoff and (b) Transmission factor as a function of COD. The assumed parabolic flow velocity profile exists for COD less than around 1×10^{-4} m and the results therefore become progressively less accurate for increasing values of COD above this point. However, in this respect, results are valid for the actual COD, which is expected to be in the range: 1.9×10^{-6} – 5.8×10^{-5} m.

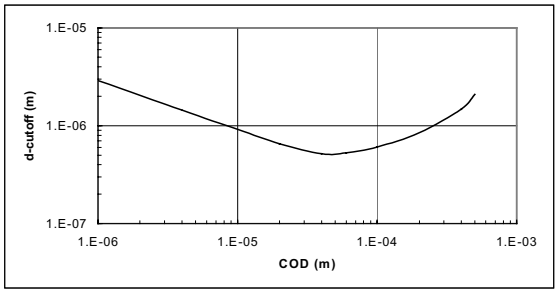

(a)

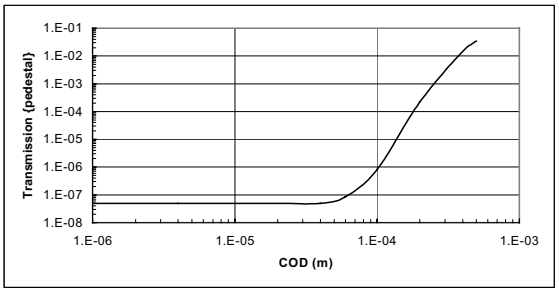

(b)

Figure 4. (a) Particle size cutoff and (b) Transmission factor as a function of COD. The assumed parabolic flow velocity profile exists for COD less than around 4×10^{-4} m and the results therefore become progressively less accurate for increasing values of COD above this point. However, in this respect, results are valid for the actual COD, which is expected to be in the range: 1.85×10^{-5} – 9.9×10^{-5} m.

3.4.2 Steel 6 cm

In this case, it is supposed that the walls of the expansion volume are constructed from 6 cm thick steel. No account it taken of any other potentially reinforcing components. This analysis, again, assumes a leak rate of 1% per day at 1 atmosphere overpressure. Figure 4 shows the particle size cutoff and transmission factor (the pedestal, or maximum attenuation, value) as a function of COD for such a barrier. Here the expected range of the COD is $1.85 \times 10^{-5} – 9.9 \times 10^{-5}$ m. Within this range the particle size cutoff falls well below 1 micron, corresponding to a transmission factor which is always below 10^{-5}. Thus, there are scenarios of interest in which such a barrier would almost totally block the aerosol arising once the particle distribution has, through coagulation, attained the characteristic size.

3.4.3 Concrete 0.5 m

For this option, the walls of the expansion volume are considered to be constituted from 0.5 m thick concrete. No account is taken of any other potentially reinforcing components. This time, a leak rate of 30% per day at 1 atmosphere overpressure is assumed. The particle size cutoff, as a function of COD, is plotted in Figure 5. Since the pedestal value of the transmission factor is always below 10^{-21} throughout this range of COD, it is not plotted, and the cutoff can be considered total. The expected COD range for this barrier construction is $1.75 \times 10^{-4} – 6.3 \times 10^{-4}$ m, and it can be seen that the cutoff diameter falls around one micron or below in this range. Since the mass median diameter for aerosols in most scenarios considered is expected to be in the range 1 – 4 micron, there is expected to be significant particle filtering in many cases.

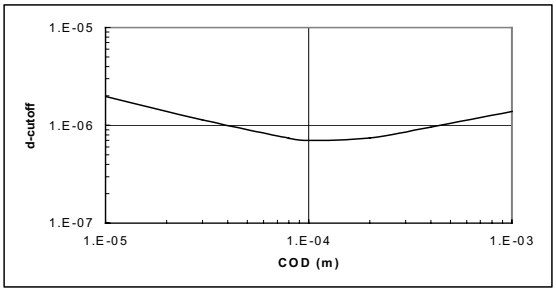

Figure 5. Particle size cutoff as a function of COD. The expected COD range is $1.75 \times 10^{-4} – 6.3 \times 10^{-4}$ m.

4. CONCLUSIONS

It has been shown that, when aerosol and environmental dispersion modelling are taken together, a more realistic treatment of the time dependence can reduce the conservatism in MEI dose estimates.

Analysis has also shown that, if the wall is sufficiently thick, significant aerosol particle filtering could occur in the cracks as material leaks across a containment barrier, such as an expansion volume. The method developed can be applied to specific scenarios, also reducing conservatism in MEI dose estimates.

ACKNOWLEDGEMENTS

This work was funded by the Office of Science and Technology and EURATOM.

REFERENCES

[1] G. Marbach, I. Cook and D. Maisonnier, The EU Power Plant Conceptual Study, *Proc. 6th International Symposium on Fusion Nuclear Technology, 7-12 April, 2002, San Diego, California, USA.*

[2] J. Raeder, I. Cook, F. H. Morgenstern, E. Salpietro, R. Bunde, E. Ebert, Safety and Environmental Assessment of Fusion Power (SEAFP): Report of the SEAFP Project, European Commission Directorate General X11, Fusion Programme, EURFUBRU X11-217/95, Brussels, June 1995.

[3] N. P. Taylor, I. Cook, C. B. A. Forty, W. E. Han and P. Taylor, "SEAFP-2 bounding accident analyses", *Fusion Engineering and Design,* **48**, *3-4*, p. 419 (2000).

[4] W. E. Han and N. P. Taylor, Calculations of temperature and mobilisation evolution for postulated accidents in SEAFP plant models, *Proc. 18th Symposium on Fusion Technology, Karlsruhe, Germany, 22-26 August 1994, Fusion Technology,* p. 1493, Elsevier (1995).

[5] W. E. Han, Monodisperse aerosol modelling for fusion power plant containments and comparison with polydisperse calculations, *Proc. 19th Symposium on Fusion Technology, Lisbon, Portugal, 16-20 September 1996, Fusion Technology,* p. 1827, Elsevier (1997).

[6] W. E. Han, "Extended Monodisperse Aerosol Modelling for Fusion Power Plant Containments", *Fusion Engineering and Design,* **42**, *1-4*, p. 127 (1998).

[7] W.E. Han, In preparation.

[8] R. H. Clarke, et al, A model for short and medium range dispersion of radionuclides released to the atmosphere, The first report of a Working Group on Atmospheric Dispersion, R. H. Clarke (Chairman), NRPB-R91.

[9] H.Boussa, et al, "A model for computation of leakage through damaged concrete structures", *Cement and Concrete Composites,* **23**, p. 279, Elsevier (2001).